Immunity, Vol. 18, 687–698, May, 2003, Copyright ©2003 by Cell Press

HDAC7, a Thymus-Specific Class II Histone Deacetylase, Regulates Nur77 Transcription and TCR-Mediated Apoptosis

Franck Dequiedt,[1] Herbert Kasler,[1] Wolfgang Fischle,[1] Veronique Kiermer,[1] Marc Weinstein,[2] Brian G. Herndier,[2] and Eric Verdin[1,3,*]

[1]Gladstone Institute of Virology and Immunology and
[2]Department of Pathology and
[3]Department of Medicine
University of California, San Francisco
San Francisco, California 94141

Summary

We report that HDAC7, a class II histone deacetylase, is highly expressed in $CD4^+CD8^+$ double-positive thymocytes. HDAC7 inhibits the expression of Nur77, an orphan receptor involved in apoptosis and negative selection, via the transcription factor MEF2D. HDAC7 is exported from the nucleus during T cell receptor activation, leading to Nur77 expression. A triple HDAC7 mutant (S155A, S318A, S448A) is not exported from the nucleus in response to TCR activation and suppresses TCR-mediated apoptosis. Conversely, a fusion of HDAC7 to the transcriptional activator VP16 activates Nur77 expression. Inhibition of HDAC7 expression by RNA interference causes increased apoptosis in response to TCR activation. These observations define HDAC7 as a regulator of Nur77 and apoptosis in developing thymocytes.

Introduction

During T cell development in the thymus, lymphocytes undergo a series of selection events. These selection processes are dependent on signals delivered by the T cell receptor (TCR) after interaction with complexes consisting of self-peptide and major histocompatibility complex (MHC). Most T cells in the thymus die by a process called "death by neglect" because they do not express a functional TCR. In contrast, T cells expressing receptors that strongly interact with self-peptide-MHC complexes are eliminated by negative selection. A minority of T cells expressing a functional TCR undergoes positive selection and further differentiation into mature T cells. A central unanswered question of T cell selection is which signals emanating from the TCR complex lead to either maturation during positive selection or to cell death during negative selection.

The orphan steroid nuclear receptor Nur77, an immediate-early gene responsive to TCR activation (Woronicz et al., 1994), has been implicated in negative selection. Overexpression of Nur77 in vivo resulted in massive apoptosis, whereas overexpression of a dominant-negative mutant inhibited TCR-mediated cell death (Calnan et al., 1995; Liu et al., 1994; Woronicz et al., 1994). Transcriptional activation of Nur77 by TCR activation is dependent on two MEF2 sites in the Nur77 promoter (Martin et al., 1994; McKinsey et al., 2002; Woronicz et al., 1995). MEF2D binds to the Nur77 promoter constitutively, irrespective of the transcriptional activity of the promoter. This observation has led to the model that MEF2D influences Nur77 promoter activity by selectively recruiting transcriptional corepressors or coactivators.

In unstimulated T lymphocytes, DNA-bound MEF2D is associated with Cabin 1, a calcineurin-interacting repressor protein (Youn et al., 1999). Cabin-1 mediates the recruitment of HDAC1 and HDAC2, which lead to the relative deacetylation of the Nur77 promoter. Cabin-1 also competes with p300 and ERK5 for MEF2D binding and prevents the recruitment of critical coactivator proteins (Kasler et al., 2000; Youn et al., 1999, 2000a, 2000b; Youn and Liu, 2000). Interestingly, a mutant mouse strain expressing a truncated Cabin-1 lacking the MEF2 binding domain showed normal thymocyte development and apoptosis (Esau et al., 2001), suggesting that other factors, besides Cabin-1, participate in the repression of Nur77 by MEF2D.

Posttranslational modifications of nucleosomal histones, in particular acetylation, are emerging as a critical mechanism in the transcriptional regulation of genes by chromatin (Strahl and Allis, 2000). The global level of histone acetylation is regulated by the antagonistic activities of histone acetyltransferases (HATs) and histone deacetylases (HDACs).

Mammalian HDACs fall into three distinct classes based on their homology to yeast proteins. Class I HDACs are homologous to the RPD3, and class II HDACs are related to HDA1, while class III HDACs are homologous to SIR2.

The class IIa HDACs, HDAC4, 5, 7, and 9, share a number of structural and functional features (reviewed in Fischle et al., 2001b; Khochbin et al., 2001). All possess a conserved C-terminal catalytic domain and interact with MEF2 proteins via a 17 amino acid motif. This interaction leads to the recruitment of class IIa HDACs to select promoters where MEF2 is bound. The repressive activity of class II HDACs is also controlled by nucleocytoplasmic shuttling and by their association with the intracellular 14-3-3 proteins in a signal-specific manner (Dressel et al., 2001; Grozinger and Schreiber, 2000; Kao et al., 2001; Zhou et al., 2001). Phosphorylation of conserved residues in the N-terminal regions of HDAC4, 5, 7, and 9 (McKinsey et al., 2000a) leads to recognition by 14-3-3 proteins, to disruption of the class II HDAC-MEF2D complexes, and to a conformational change leading to nuclear export (McKinsey et al., 2001b). The functional relevance of these findings has been elegantly illustrated in muscle development (reviewed by McKinsey et al., 2001a; Wang et al., 2000).

Here, we show that HDAC7, a class II HDAC, is expressed at high levels in $CD4^+CD8^+$ double-positive thymocytes. HDAC7 represses the expression of Nur77 by interacting with MEF2D in the nucleus and plays an important role in the regulation of Nur77 expression and apoptosis in response to T cell activation.

Results

High HDAC7 Expression in Human Thymus

Analysis of human tissues by Northern blot with a human HDAC7 probe showed a major transcript (4.4 kb) and a

*Correspondence: everdin@gladstone.ucsf.edu

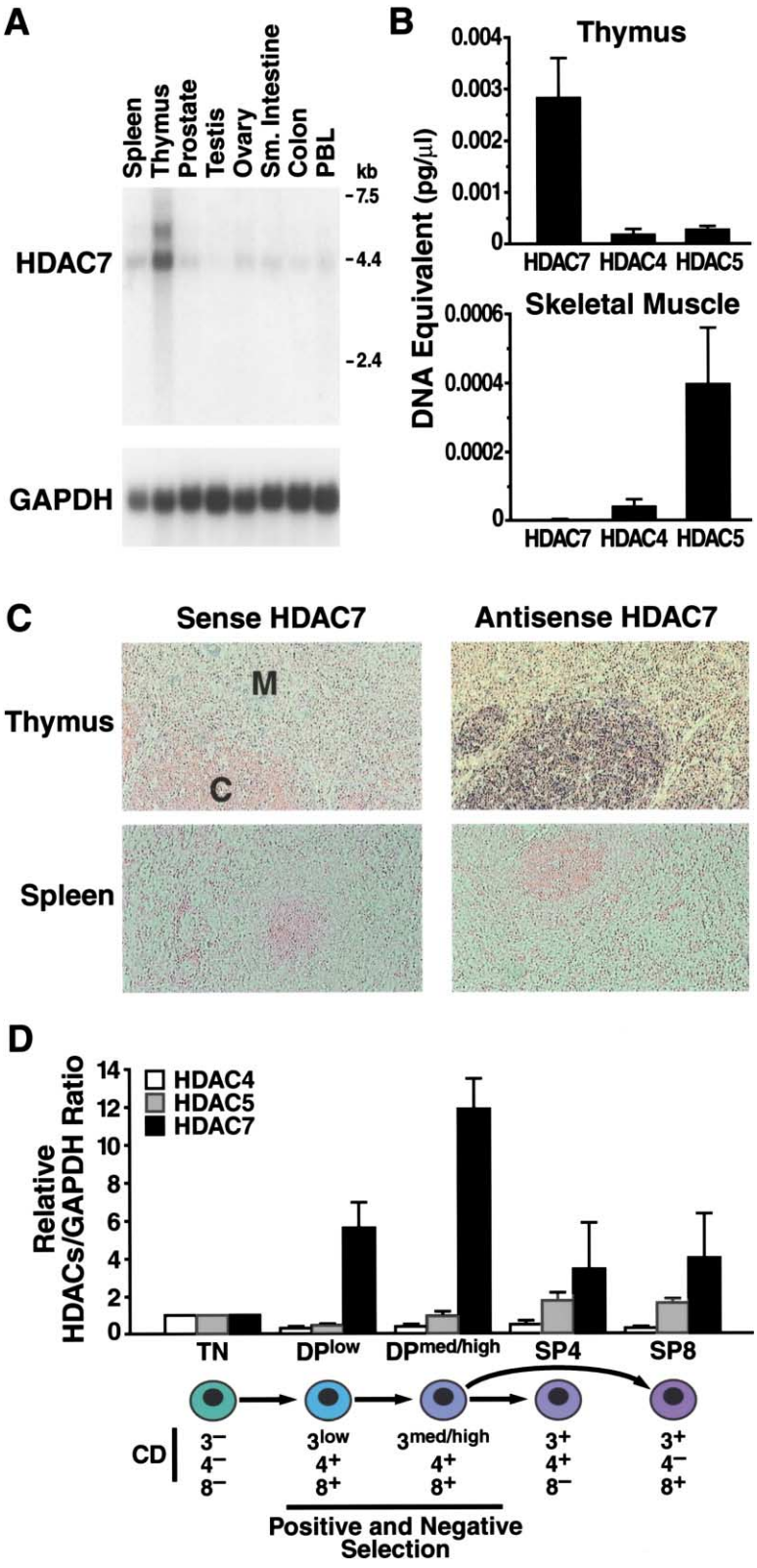

Figure 1. Human HDAC7 Is Highly Expressed in Double-Positive Thymocytes

(A) A multiple human tissue Northern blot (Clontech) was probed with a human HDAC7 ^{32}P-radiolabeled cDNA probe. The same membrane was hybridized with a probe corresponding to human GAPDH cDNA. Molecular size markers are indicated on the right.

(B) Real-time PCR was used to assess expression levels of HDAC4, HDAC5, and HDAC7 in thymus and skeletal muscle. Expression levels are shown relative to a standard curve established from dilutions of plasmid DNA corresponding to each cDNA.

(C) Thymic and spleen sections were hybridized with a sense or an antisense RNA corresponding to HDAC7. After incubation, slides were developed and counterstained with nuclear fast red. The locations of the cortical (C) and medullar (M) regions of the thymus are indicated.

(D) Thymocytes were sorted based on surface expression of CD3, CD4, and CD8 into triple-negative (TN), double-positive (DP), and single-positive (SP4 and SP8). Expression of class II HDACs was assessed in each subset by real-time RT-PCR and normalized to GAPDH expression. Class II HDAC mRNA abundance for HDAC4 (white bars), HDAC5 (gray bars), and HDAC7 (black bars) is plotted relative to mRNA levels in triple-negative thymocytes (TN).

minor transcript (6.0 kb) in human thymus (Figure 1A). Dot blot analysis of more than 40 different human tissues confirmed that samples corresponding to adult and fetal thymus showed highest levels of HDAC7 mRNA (data not shown).

Comparative analysis of relative expression levels of

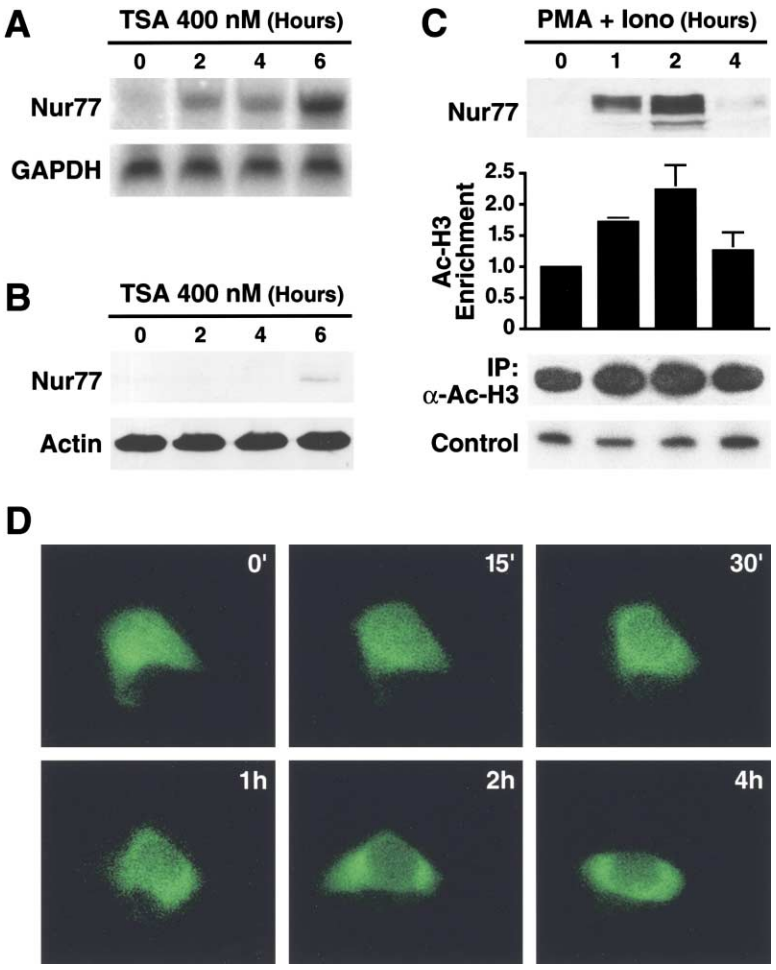

Figure 2. Regulation of Nur77 Transcription by Histone Acetylation

(A) DO11.10 cells were treated with 400 nM TSA, and expression of Nur77 was analyzed over time by Northern blot. The same blot was hybridized with a GAPDH probe as a control.

(B) Total cellular extracts from DO11.10 cells treated with TSA were analyzed by Western blotting with an anti-Nur77 antibody. The same extracts were analyzed with an antiserum for actin as control.

(C) DO11.10 cells were activated with PMA/ionomycin for 0, 1, 2, and 4 hr. Nuclear lysates were incubated with an antibody against acetylated histone H3. Immunoprecipitated DNA was amplified by PCR with specific primers for the Nur77 promoter. Results are represented as histogram of the relative enrichment (immunoprecipitated/input) in DNA associated with acetylated histone H3 relative to untreated cells.

(D) Cells transfected with HDAC7-GFP were activated with PMA/ionomycin. Subcellular localization of HDAC7 was followed with real-time immunofluorescence microscopy after 0, 15, and 30 min, and 1, 2 and 4 hr of treatment.

HDAC7, HDAC4, and HDAC5 by real-time polymerase chain reaction (PCR) showed that HDAC7 was significantly more abundant than HDAC4 and HDAC5 in human thymus (Figure 1B). The opposite was observed in skeletal muscle where HDAC7 levels were below the detection limit while HDAC4 and HDAC5 were readily detected.

We used in situ hybridization with HDAC7 sense and antisense RNA probe to determine the precise location of HDAC7 expression within the thymus. Cells of lymphoid morphology containing high levels of HDAC7 transcripts were abundant in the cortical region of the thymus (Figure 1C). No signal was detected with the sense probe on thymic sections or with either probe on spleen samples (Figure 1C).

To determine the expression pattern of HDAC7 during thymocyte maturation, we sorted human primary thymocytes by flow cytometry based on the expression of differentiation markers CD3, CD4, and CD8. The relative abundance of HDAC4, HDAC5, and HDAC7 mRNAs was assessed by real-time PCR in each population. Low levels of HDAC7 mRNA were observed in immature triple-negative thymocytes (TN, $CD3^-CD4^-CD8^-$) (Figure 1D). HDAC7 expression was highly and transiently increased during the $CD4^+CD8^+$ double-positive (DP) stage and returned to lower levels in mature single-positive T cells (SP4 or SP8). Within the DP thymocytes population, expression of HDAC7 was higher in the more mature $CD3^{med/high}$ subpopulations. In contrast, HDAC4 and HDAC5 expression was moderately downregulated during the DP stage (Figure 1D). These observations demonstrate the selective upregulation of HDAC7 expression in DP thymocytes.

Transcriptional Activity of Nur77 Is Regulated by Histone Acetylation

Since class II HDACs and members of the MEF2 family interact functionally in muscle development, we hypothesized that HDAC7 could interact with MEF2D to modulate Nur77 promoter activity in developing thymocytes. First, we assessed the role of histone acetylation on the transcriptional activity of the Nur77 promoter. A T cell hybridoma cell line (DO11.10) was treated with an HDAC inhibitor, trichostatin A (TSA), and expression of Nur77 was assessed by Northern blot analysis. Nur77 mRNA was induced in a time-dependent manner after addition of TSA to the culture medium (Figure 2A). Similar results were obtained by Western blot analysis using a Nur77-specific antiserum (Figure 2B). These data suggest that the Nur77 promoter is suppressed under basal conditions by the activity of an HDAC.

To assess directly the levels of histone acetylation in the Nur77 promoter during TCR activation, we performed chromatin immunoprecipitation (ChIP) experi-

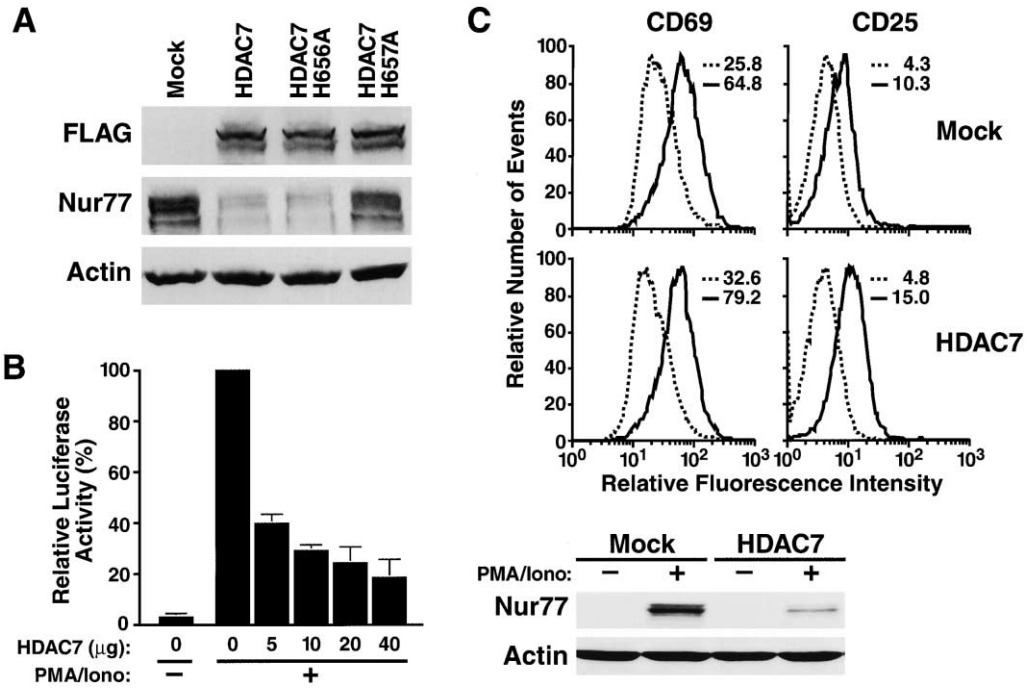

Figure 3. HDAC7 Represses Nur77 Promoter Activity

(A) Total cellular lysates were prepared from polyclonal DO11.10 cells stably expressing FLAG-tagged versions of wild-type HDAC7, HDAC7 H656A, HDAC7 H657A, or pCDNA3.1 (Mock); cells were treated with PMA/ionomycin for 1.5 hr. Cell lysates were analyzed by Western blotting with antisera for Nur77, FLAG, and actin.

(B) D011.10 cells were transfected with the pNur77-Luc reporter construct and increasing amounts of HDAC7 expression vector. Luciferase activity was measured in cells treated with PMA/ionomycin for 4 hr (+) and in untreated cells (−). Results are from three independent experiments each in triplicate. The activity of the Nur77 promoter is expressed relative to its activity after PMA/ionomycin treatment in mock-transfected cells.

(C) Polyclonal cell lines expressing HDAC7 or the empty vector (Mock) were stimulated with PMA/ionomycin. Surface expression of CD69 and CD25 was measured by flow cytometry before (dotted line) and 2 hr (CD69) or 8 hr (CD25) after treatment (solid line). Western blot analysis of the same cells for Nur77 expression confirms that HDAC7 expression leads to a suppression of Nur77 induction.

ments. DO11.10 cells were activated with phorbol myristate acetate (PMA) and ionomycin, a treatment that mimics signaling by the TCR-CD3 complex. Nur77 protein levels increased in the first 2 hr after addition of PMA and ionomycin and decreased at 4 hr (Figure 2C). In parallel, acetylated histone H3 was immunoprecipitated from chromatin solution, and the presence of Nur77 promoter sequences was analyzed by PCR. This analysis revealed that the Nur77 promoter became relatively enriched in acetylated histone H3 during the first 2 hr after induction and returned to basal levels by 4 hr after induction, in close parallel to the Nur77 protein (Figure 2C).

The transcriptional repression mediated by Class II HDACs is regulated, in part, via their nucleo-cytoplasmic localization. To determine the subcellular localization of HDAC7, we transfected DO11.10 cells with an HDAC7-GFP fusion construct. Using real-time immunofluorescence microscopy on live cells, we observed that unactivated DO11.10 cells showed predominantly nuclear HDAC7 (Figure 2D). Fifteen minutes after addition of PMA/ionomycin, HDAC7 was observed relocating to the cytoplasm. Exclusion of HDAC7 from the nucleus was complete after 30 min, in agreement with the kinetics of Nur77 induction after PMA/ionomycin (Figure 2C). These results indicate that Nur77 transcription is regulated by acetylation and suggest that HDAC7 could be involved in this mechanism.

HDAC7 Suppresses Induction of Nur77 by TCR Signaling

To determine whether HDAC7 can suppress the transcriptional activity of the endogenous Nur77 promoter, we generated polyclonal cell lines stably expressing HDAC7 or HDAC7 mutants (H656A and H657A). The H657A mutation abolished enzymatic activity of HDAC7 while the H656A mutation had no effect, as expected based on our recent mutational analysis of HDAC4, a closely related protein (Fischle et al., 2002). DO11.10 cells were infected with a retrovirus expressing HDAC7 or HDAC7 mutants and green fluorescent protein (GFP) from a polycistronic mRNA in which the two open reading frames are separated by an internal ribosome entry site. Transduced cells were sorted by flow cytometry based on GFP expression and activated by treatment with PMA/ionomycin. Nur77 protein induction was strongly inhibited by wild-type HDAC7 and by the catalytically active H656A mutant but not by the catalytically inactive H657A mutant (Figure 3A).

Next, we examined the effect of HDAC7 on the transcriptional activity of the isolated Nur77 promoter in a reporter assay (Woronicz et al., 1995). PMA/ionomycin treatment increased the activity of the transfected Nur77-promoter construct by 100-fold (Figure 3B). Expression of HDAC7 inhibited Nur77 promoter activity in a dose-dependent manner (Figure 3B).

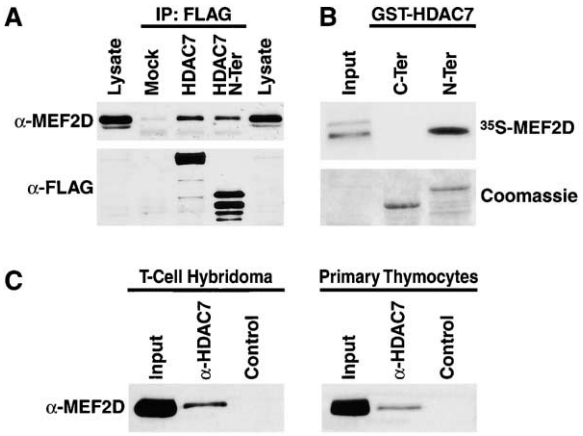

Figure 4. HDAC7 and MEF2D Interact In Vivo

(A) Total cellular extracts prepared from DO11.10 cell lines stably expressing HDAC7 or its amino terminus were immunoprecipitated with anti-FLAG antiserum and analyzed by Western blotting with an antibody against MEF2D (αMEF2D). The immunoprecipitated material was analyzed in parallel by Western blotting with an anti-FLAG antiserum (αFLAG). Input equals 10% of the lysate used in the immunoprecipitation.

(B) Binding of MEF2D to the carboxyl (C-ter) or amino (N-ter) terminus of HDAC7 was measured in pull-down assays with in vitro translated ^{35}S-labeled MEF2D. Input corresponds to 10% of the material used for pull-down.

(C) Total cellular extracts from DO11.10 cells or primary thymocytes were immunoprecipitated with an antiserum specific for HDAC7 or an isotype control. Immunoprecipitated material was analyzed by Western blotting with an antiserum against MEF2D (α-MEF2D).

To demonstrate the specificity of Nur77 inhibition by HDAC7, we examined two other markers of T cell activation, CD69 (early) and CD25 (late), in T cell hybridoma transduced with HDAC7 or the empty vector. Both CD69 and CD25 were induced to the same degree in response to PMA/ionomycin, independently of HDAC7 expression (Figure 3C). As expected, induction of Nur77 was inhibited in the cell line expressing HDAC7 (Figure 3C, lower panel). These results indicate that HDAC7 specifically represses Nur77 transcription.

HDAC7 Interacts with MEF2D via Its Amino Terminus

Class II HDACs interact with members of the MEF2 family via a small domain located in their amino terminus. To determine whether HDAC7 interacts with MEF2D, we generated stable polyclonal cell lines expressing FLAG-tagged HDAC7 or its amino-terminal domain (amino acids 1–487). HDAC7 was immunoprecipitated with an anti-FLAG antibody, and the presence of endogenous MEF2D was detected by Western blot analysis. Both full-length HDAC7 and its amino-terminal domain specifically coimmunoprecipitated with endogenous MEF2D (Figure 4A).

To test whether this interaction was direct or indirect, we expressed the N- (aa 1–488) and C-terminal (aa 438–915) regions of HDAC7 as GST fusion proteins in *E. coli* and tested their ability to interact with in vitro translated MEF2D. MEF2D bound to the N-terminal but not to the C-terminal fragment of HDAC7 (Figure 4B).

Finally, endogenous MEF2D coimmunoprecipitated with HDAC7 in both T cell hybridomas and primary thymocytes, whereas the isotype control immunoprecipitation showed no associated MEF2D protein (Figure 4C).

These results are consistent with the hypothesis that HDAC7 is recruited to the Nur77 promoter through an interaction with MEF2D.

Interaction of HDAC7 with MEF2D Is Essential for Repression of Nur77

Both HDAC4 and HDAC5 interact with MEF2 proteins via a conserved motif of 17 amino acids located in the amino-terminal region of the proteins (Figure 5A). To determine the possible function of this motif, we generated mutants of HDAC7 by deleting the entire 17 amino acid stretch (Figure 5A, HDAC7-ΔMEF) or by substituting several residues with alanine residues (HDAC7-K86AK88A and HDAC7-Q87AE91A) (Figure 5A). HDAC7 and mutants were synthesized and labeled in vitro and tested for their ability to interact with GST-MEF2D fusion protein in pull-down experiments. HDAC7 specifically interacted with GST-MEF2D but not with GST alone (Figure 5B). In contrast, HDAC7-ΔMEF and HDAC7-K86AK88A did not interact with MEF2D, while the double mutant HDAC7 Q87AE91A retained the capacity to interact with MEF2D (Figure 5B). To confirm these observations in vivo, we transduced FLAG-tagged versions of these HDAC7 expression vectors into DO11.10 cells. After establishment of polyclonal cell lines, stably expressed proteins were immunoprecipitated with an anti-FLAG antibody and assessed for binding to endogenous MEF2D. In agreement with in vitro experiments, HDAC7 and the HDAC7-Q87AE91A mutant interacted with endogenous MEF2D while the HDAC7-ΔMEF and HDAC7-K86AK88A mutants showed no MEF2D binding (Figure 5C).

To determine the functional role of the MEF2D-HDAC7 interaction, we tested the HDAC7 mutants for their ability to repress the Nur77 promoter. Expression of the HDAC7 mutants defective for MEF2D binding (HDAC7-ΔMEF and HDAC7-K86AK88A) had no effect on Nur77 promoter activity in transfection assays (Figure 5D). In contrast, both wild-type HDAC7 and the HDAC7-Q87AE91A mutant inhibited transcriptional activation of the Nur77 reporter (Figure 5D). Next, polyclonal cell lines stably expressing each mutant were obtained after transduction of DO11.10 cells. In agreement with our transfection experiments, HDAC7 mutants unable to interact with MEF2D (HDAC7-ΔMEF and HDAC7-K86AK88A) failed to repress endogenous Nur77 expression (Figure 5E). These experiments demonstrate that the HDAC7-MEF2D interaction is necessary for HDAC7 to repress Nur77 transcription.

The Nur77 Promoter Is Transactivated by a Fusion Protein Between HDAC7 and the VP16 Transactivating Domain

To further demonstrate the specific recruitment of HDAC7 to the Nur77 promoter, we fused the N terminus of HDAC7 or of a mutant lacking the MEF2D interaction domain to the herpes simplex virus VP16 transactivation domain (Nter-VP16 and NterΔMEF-VP16, Figure 6A). Both constructs were independently transfected in DO11.10 cells with pRSRFwt-Luc, a reporter construct containing four MEF2D DNA binding sites derived from

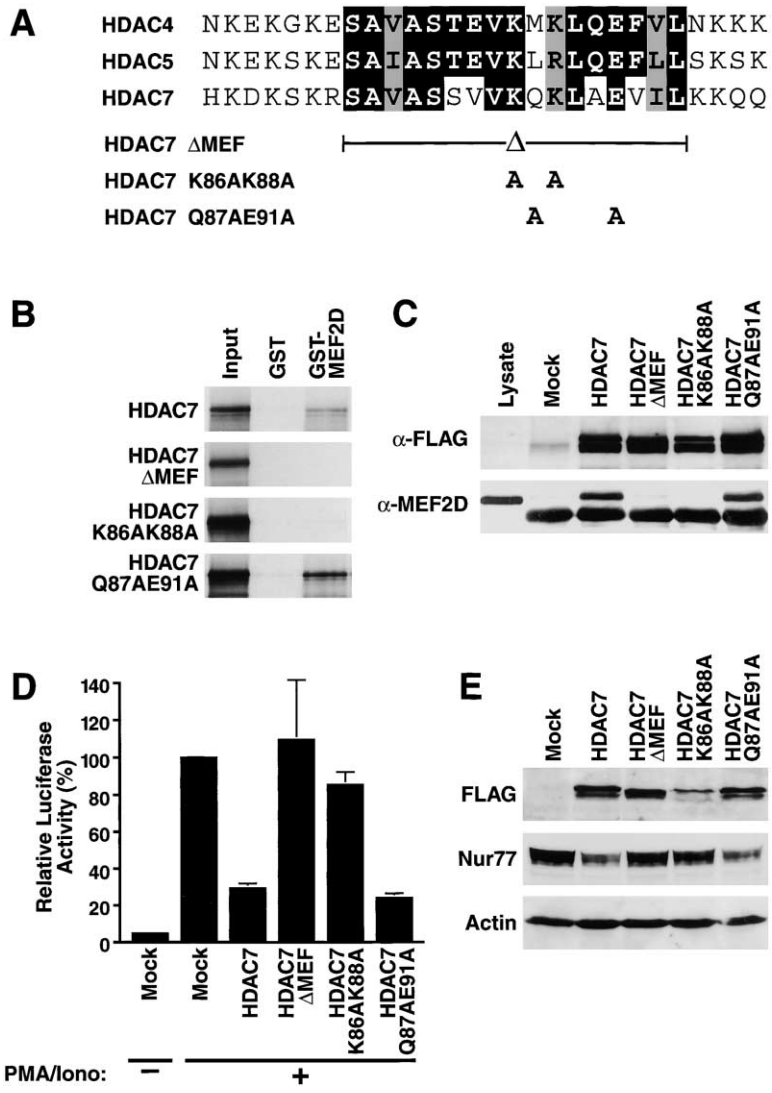

Figure 5. Interaction of HDAC7 with MEF2D Is Necessary for Repression of Nur77 Expression

(A) Sequence comparison of the MEF2D binding domain of HDAC4, HDAC5, and HDAC7 (conserved residues are in black; semiconserved residues in gray).

(B) Binding of HDAC7 and mutants to GST-MEF2D was tested in a pull-down assay with in vitro translated ^{35}S-labeled MEF2D. The input amount is equal to 10% of the material used in the pull-down.

(C) HDAC7 and mutants were stably expressed in DO11.10 cells. Total cellular lysates were immunoprecipitated with an anti-FLAG antiserum and analyzed by Western blot with specific antisera for MEF2D (α-MEF2D) and the FLAG epitope as control (α-FLAG). Input equals 10% of the lysate used in the immunoprecipitation. The lower band represents the light chain from mouse IgGs used in the immunoprecipitation.

(D) D011.10 cells were cotransfected with pNur77-Luc and the indicated HDAC7 expression vectors and activated with PMA/ionomycin for 4 hr. Luciferase activity was measured in treated (+) and untreated (−) cells. The results are from three independent experiments each in triplicate. The activity of the Nur77 promoter is expressed relative to its activity after PMA/ionomycin treatment in mock-transfected cells.

(E) Total cellular lysates were prepared from polyclonal DO11.10 cells stably expressing FLAG-tagged versions of wild-type HDAC7, HDAC7-ΔMEF, HDAC7-K86AK88A, HDAC7-Q87AE91A, or pCDNA3.1 (Mock), treated with PMA/ionomycin for 1.5 hr. Cell lysates were analyzed by Western blotting with antisera for Nur77, FLAG, and actin.

the Nur77 promoter (Figure 6B, gray bars). As a control, a pRSRFmut-Luc construct containing mutated ME2D binding sites was used (Figure 6B, black bars). Cotransfection of pRSRFwt-Luc with Nter-VP16 yielded transcriptional activation at levels similar to those obtained with PMA/ionomycin. In contrast, the NterΔMEF-VP16 protein had no effect on pRSRFwt-Luc, indicating that the interaction of MEF2D with the amino terminus of HDAC7 is critical. As expected, the pRSRFmut-Luc construct was unaffected by all treatments (Figure 6B).

Next, we measured the expression of endogenous Nur77 in cells transfected with Nter-VP16 using Northern blot analysis. The Nur77 message was barely detectable in cells transfected with the control vector and was strongly activated in response to PMA/ionomycin, as previously reported (Figure 6C) (Woronicz et al., 1995). Transfection of the Nter-VP16 construct, but not NterΔMEF-VP16 or the empty vector (FLAG-VP16), activated endogenous Nur77 expression (see Figure 6C). Similar results were obtained by measuring the activity of a Nur77-dependent promoter (NBRE-Luc) after transfection (Figure 6D, gray bars). As expected, an NBRE-luc construct containing mutated Nur77 binding sites was not affected by any of the constructs (Figure 6D, black bars).

A Phosphorylation Mutant HDAC7 Suppresses Nur77 Induction in Response to TCR Activation

Phosphorylation of serine residues in the amino terminus of class IIa HDACs is required for their nuclear export to the cytoplasm (Wang et al., 2000; Kao et al., 2001; Zhang et al., 2001; Miska et al., 2001; McKinsey et al., 2000a, 2000b; Grozinger and Schreiber, 2000). Each of these conserved serine residues was mutated to an alanine individually (S155A, S318A, and S448A) or as a combined triple mutant (ΔP). Constructs containing a single mutated serine (S155A, S318A, and S448A) inhibited Nur77 transcriptional activity slightly better than wild-type HDAC7 (Figure 7A). However, the triple mutant (HDAC7-ΔP) almost totally abolished induction of Nur77 transcription by PMA/ionomycin treatment.

To assess the subcellular localization of the triple phosphorylation mutant, we transfected an HDAC7ΔP-GFP construct into DO11.10 cells (Figure 7B). In unstimulated cells, HDAC7ΔP localized mainly in the nucleus, similar to HDAC7. As expected, wild-type HDAC7 was

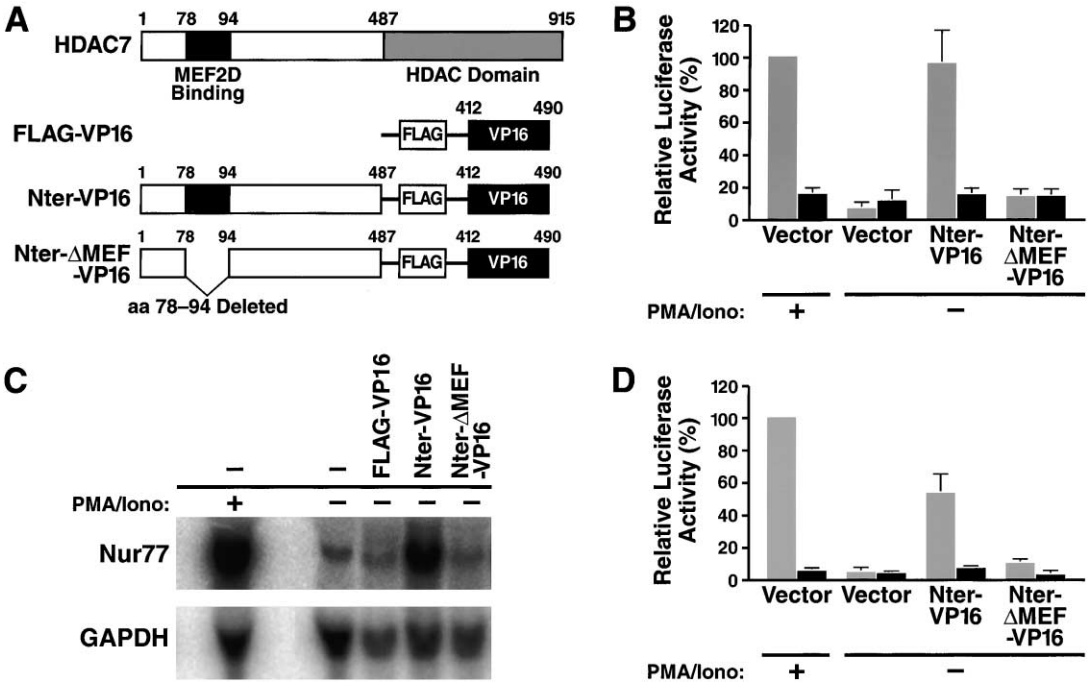

Figure 6. Induction of Nur77 Expression by HDAC7-VP16 Fusion Proteins

(A) Schematic representation of wild-type (HDAC7) and modified versions of HDAC7, Nter-VP16, and NterΔMEF-VP16.

(B) Fusion constructs schematized in (A) were cotransfected in DO11.10 with pRSRF-Luc. Luciferase activities are shown relative to the luciferase activity measured after 4 hr of treatment with PMA/ionomycin (100%). Gray bars correspond to the wild-type pRSRFwt-Luc and dark bars to pRSRFmut-Luc.

(C) VP16-fusion constructs schematized in (A) were transfected in DO11.10, and Nur77 was detected by Northern blot. Hybridization with a human GAPDH probe is shown as a control for equal RNA loading.

(D) Fusion constructs schematized in (A) were cotransfected in DO11.10 with pNBRE-Luc. Luciferase activities are shown relative to the luciferase activity measured after 4 hr of treatment with PMA/ionomycin (100%). Gray bars correspond to the wild-type pNBREwt-Luc and dark bars to pNBREmut-Luc.

exported out of the nucleus following stimulation with PMA/ionomycin or α-CD3 antibodies (Figure 7B). In contrast, HDAC7ΔP remained nuclear in response to the same treatments (Figure 7B).

Next, we assessed the ability of HDAC7ΔP to repress the induction of endogenous Nur77. Cells treated with PMA/ionomycin had elevated Nur77 expression which was weakly inhibited in cells transduced with HDAC7 and completely suppressed in response to HDAC7ΔP (HDAC7ΔP, Figure 7C). These observations were confirmed using a Nur77-dependent reporter construct (pNBRE-Luc). Despite being expressed at significantly lower levels than HDAC7, HDAC7ΔP led to complete suppression of promoter activity while HDAC7 only led to partial inhibition (Figure 7D).

HDAC7 Modulates the Rate of Thymocyte Apoptosis in Response to TCR Signaling

These observations suggested that HDAC7 could regulate thymocyte apoptosis following TCR engagement. First, we tested whether overexpression of HDAC7ΔP inhibits TCR-mediated apoptosis. We used cells stably transduced with HDAC7 or HDAC7ΔP and measured their apoptosis rate in response to PMA/ionomycin or αCD3 antibody (Figure 8A). High levels of apoptosis were detected in the control cell line transduced with empty vector following a 24 hr treatment with PMA/ionomycin or αCD3 antibody (Figure 8A, Mock). Overexpression of HDAC7 weakly inhibited apoptosis induced by PMA/ionomycin or αCD3 antibodies (Figure 8A, HDAC7). In contrast, overexpression of HDAC7ΔP was associated with significantly stronger inhibition of apoptosis (Figure 8A). Importantly, this protective effect was not observed when cell death was induced by dexamethasone (data not shown).

Next, we predicted that suppression of HDAC7 expression should lead to an increase in apoptosis in response to TCR activation. We used a murine stem cell virus (MSCV)-based retroviral vector to introduce a small hairpin RNA (shRNA) specific for either HDAC7 or for GL3 luciferase in DO11.10 cells. Western blot analysis of cells transduced with these vectors revealed that the HDAC7-specific shRNA inhibited HDAC7 expression to undetectable levels while the GL3 luciferase shRNA was without effect (Figure 8B, right panel). In agreement with our model, the cell line containing the HDAC7-specific shRNA showed increased apoptosis in response to α-CD3 antibody over a range of concentrations (Figure 8B, left panel). These observations demonstrate that HDAC7 expression modulates the apoptosis rate of T cells in response to T cell activation signals.

Discussion

We report here that HDAC7 represses Nur77 expression and modulates the rate of apoptosis of T cells in re-

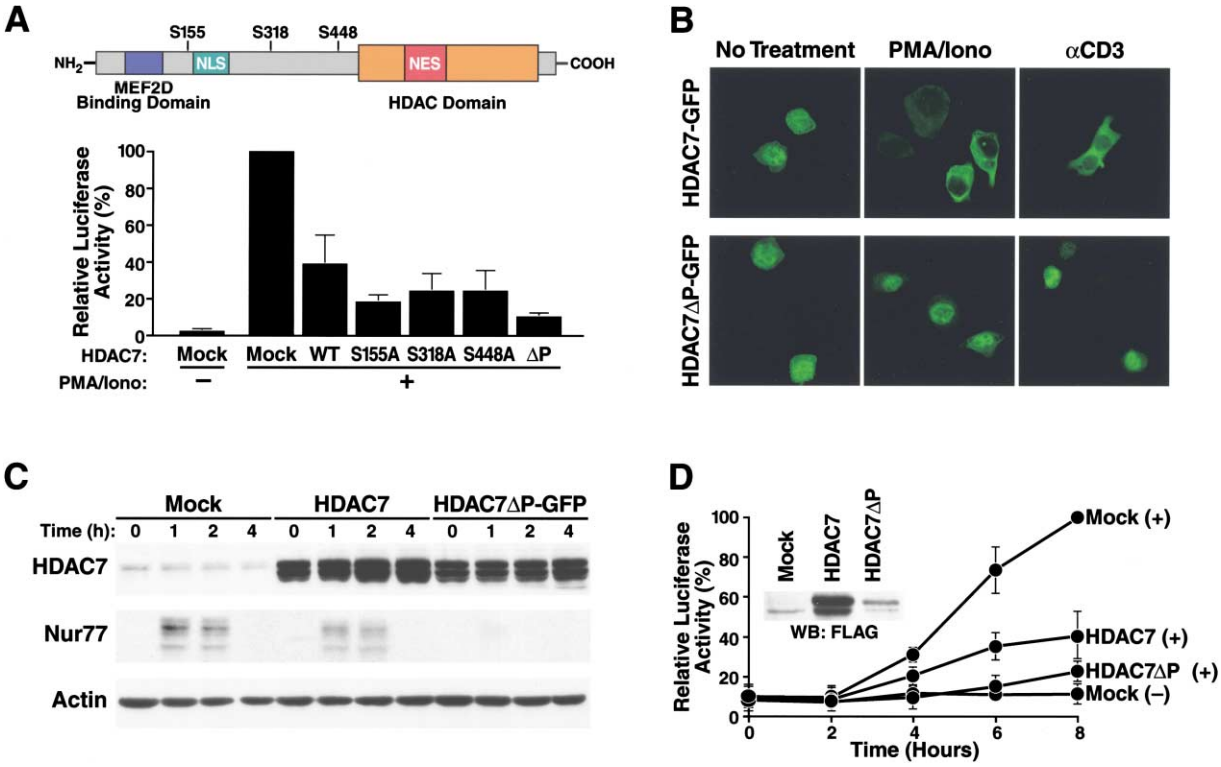

Figure 7. Superrepression of Nur77 Expression by a Nuclear-Export-Defective HDAC7

(A) Schematic representation of HDAC7. The MEF2D interaction motif, the nuclear localization signal (NLS), the nuclear export signal (NES), and the positions of phosphorylated serines are indicated. D011.10 cells were transfected with the pNur77-Luc reporter construct and the same quantity of empty vector (Mock), wild-type HDAC7 (WT), or the indicated mutant (S155A, S318A, S448A, or ΔP) expression vector, and activated with PMA/ionomycin for 4 hr. Luciferase activity was measured in treated (+) and untreated (−) cells. The results are from three independent experiments each in triplicate. The activity of the Nur77 promoter is expressed relative to its activity after PMA/ionomycin treatment in mock-transfected cells.

(B) DO11.10 cells were transfected with HDAC7-GFP or HDAC7ΔP-GFP. Cells were untreated or treated with PMA/ionomycin or αCD3 antibodies 24 hr posttransfection. Intracellular localization of GFP-fusion proteins was monitored by immunofluorescence microscopy after 2 hr of treatment.

(C) Total cellular lysates were prepared from polyclonal DO11.10 cells stably expressing FLAG-tagged versions of wild-type HDAC7, HDAC7ΔP, or empty vector (Mock) and treated with PMA/ionomycin for 0, 1, 2, or 4 hr. Cell lysates were analyzed by Western blotting with antisera for Nur77, HDAC7, and actin.

(D) Expression vectors for either wild-type HDAC7, HDAC7ΔP, or empty vector (Mock) were cotransfected in DO11.10 with pNBREwt-Luc. Luciferase activities were measured after 0, 2, 4, 6, and 8 hr in PMA/ionomycin-treated cells (+) or untreated cells (−) as control. Results are presented relative to the luciferase activity measured after 8 hr of treatment in the mock-transfected cells (100%).

sponse to TCR engagement. Previous work identified Cabin-1, a MEF2D binding protein, as an inhibitor of Nur77 expression and TCR-mediated apoptosis (Youn and Liu, 2000; Youn et al., 1999). However, deletion of the MEF2D interacting domain of Cabin-1 did not affect T cell apoptosis in mice, an observation compatible with the existence of redundant regulatory processes (Esau et al., 2001).

Two distinct models can account for these observations. First, both Cabin-1 and HDAC7 could be coexpressed at the same stage in thymocyte development. When present in the same cell, HDAC7 and Cabin-1 could be acting simultaneously to ensure a strict control of Nur77 expression. These multiple repressors would ensure that activation of Nur77 transcription happens only when proper signaling cascades converge in the nucleus of the developing thymocyte and inactivate both repressors. The expression of two distinct repressors in the same cell may reflect the importance of avoiding inappropriate expression of the Nur77 death gene during thymic development of T cells.

As an alternative model, HDAC7 and Cabin-1 could control Nur77 activation by TCR stimulation at discrete stages during thymocyte maturation, each repressor ensuring the silencing of Nur77 expression at a distinct developmental stage. While Cabin-1 is ubiquitously expressed, HDAC7 is predominantly expressed in double-positive thymocytes, where negative selection via TCR signaling occurs.

Independently of the repressor mechanism, previous observations and data presented in this manuscript support the model that the level of histone acetylation in the Nur77 promoter is an important determinant of its transcriptional activity. MEF2D-associated Cabin-1 represses Nur77 transcriptional activity partly by recruiting HDAC1 and -2 via Sin3 (Youn and Liu, 2000). We observed that HDAC7 is recruited to the Nur77 promoter via its interaction with MEF2D and inhibits transcription through its deacetylase activity. We provide direct experimental evidence that TCR activation of Nur77 transcription is accompanied by local hyperacetylation of histones. Furthermore, treatment of thymocytes with the

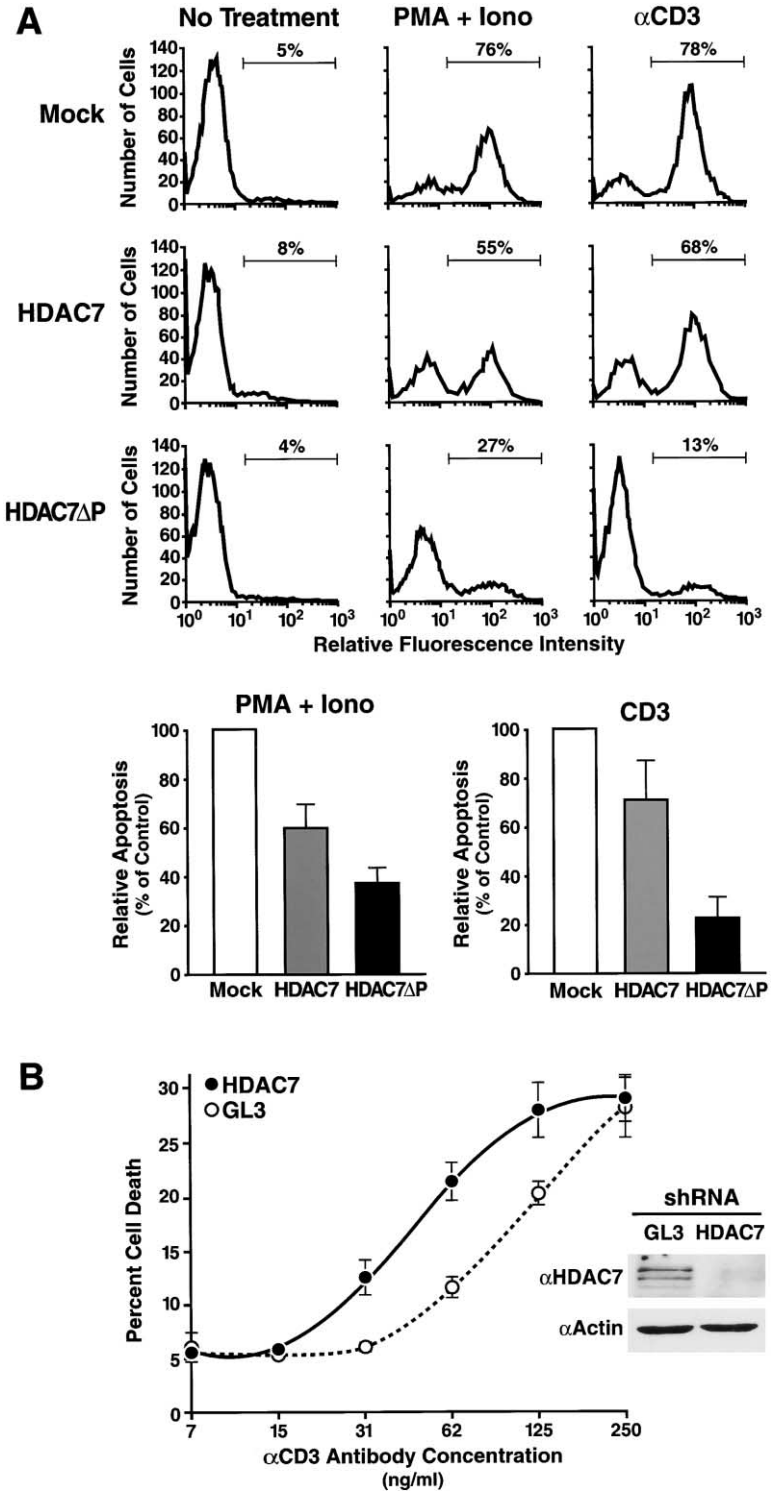

Figure 8. HDAC7 Regulates Thymocyte Apoptosis in Response to TCR Engagement

(A) Polyclonal DO11.10 cell lines, stably expressing HDAC7, HDAC7ΔP, or the empty vector (Mock), were stimulated with PMA/ionomycin or αCD3 antibodies. Apoptotic cells were detected after 24 hr by phycoerythrin-annexin V staining and flow cytometry analysis. Flow histograms illustrate the percentages of apoptotic cells detected in a representative experiment. Bar histograms represent the mean apoptotic rates from four independent experiments and are expressed relative to the apoptotic rate observed in the mock-transduced cell line (100%).

(B) Polyclonal cell lines transduced with shRNA for either HDAC7 or GL3 luciferase were incubatd for 13 hr in wells precoated with αCD3 ϵ (Pharmingen, clone 500A2; 7, 15, 31, 62, 125, and 250 ng/ml) and αCD28 (Pharmingen, clone 37.51, 1 μg/ml) antibodies and assayed for apoptosis. Results shown are representative of three separate experiments, each performed in triplicate. Difference in apoptosis between the two cell populations are significant at antibody concentrations of 31, 62, and 125 ng/ml ($p < 0.01$).

histone deacetylase inhibitor TSA alone activates the Nur77 promoter. This observation indicates that the Nur77 promoter belongs to a small fraction of cellular promoters (2% or less) that are under the dominant control of a repressive HDAC and can be activated solely by inhibition of HDAC activity (Van Lint et al., 1996).

According to current models of T cell maturation, thymic negative and positive selections are directly dependent on signals delivered by the activation of the TCR. Cells that express a functional TCR undergo either positive or negative selection. Based on our observations, we speculate that HDAC7 plays a critical role in determining the threshold level at which a developing T cell undergoes positive versus negative selection. HDAC7 could allow some level of TCR activation without a concomitant increase in Nur77 expression, a situation that

might allow for positive selection to occur. When the TCR signal is sufficiently strong, the suppressive effect of HDAC7 on Nur77 expression would be overwhelmed, resulting in Nur77 expression and negative selection via apoptosis. According to this model, HDAC7 therefore might serve as a rheostat modulating the apoptotic response of developing thymocytes in response to TCR activation. Our observations that overexpression of HDAC7 inhibits apoptosis and that inhibition of HDAC7 expression via shRNA enhances apoptosis support this model. Future experiments in transgenic mice will directly test this hypothesis and further define the role of HDAC7 in thymic T cell selection.

Experimental Procedures

Plasmids

The pcDNA3.1-based expression vector for FLAG-tagged human HDAC7 has been described elsewhere (Fischle et al., 2001a). C-terminal green fluorescence protein fusions were constructed in peGFP-N1 (Clontech). Deletion constructs of HDAC7 were generated by PCR and cloning procedures as described (Fischle et al., 2001a). Site-directed mutagenesis was performed with the QuikChange kit (Stratagene). All mutations were verified by DNA sequencing. To construct N-terminal GST-fusion proteins, EcoRI fragments from the pcDNA3.1 expression constructs were subcloned into the EcoRI site of pGEX4T1 (Pharmacia). The luciferase reporter plasmid driven by the Nur77 promoter (pNur77-Luc) was generated by cloning the −3800 to +87 genomic sequences of the Nur77 promoter (a kind gift from Astar Winoto, University of California, Berkeley) (Woronicz et al., 1995) into pGL2 basic (Promega). Mouse MEF2D was also received from Winoto's lab. Minimal MEF2 wild-type and mutant reporter constructs (pRSRFwt-Luc and pRSRFmut-Luc) are described elsewhere (Woronicz et al., 1995).

Cell Culture, Transfections, and Reporter Assay

DO11.10 T cell hybridomas were grown at 37°C in RPMI 1640 medium supplemented with 10% fetal bovine serum, 2 mM glutamine, and 50 U/ml streptomycin/penicillin. Transfections were performed by the DEAE-dextran-chloroquine method. The DNA concentration was kept constant in the different samples by using the corresponding empty vector. In some cases, cells were treated with PMA (10 ng/ml) and ionomycin (0.5 μM) for 4 hr, beginning 16 hr after transfection, and harvested for reporter assays. All transfections were done in triplicate and are presented as the result of at least three independent experiments. Luciferase reporter assays were done with the dual luciferase reporter assay system (Promega) using an EF1α promoter-driven *Renilla* luciferase expression vector as an internal control.

For all α-CD3 stimulation (except in Figure 8C), monoclonal antibody 500A2 was bound to the culture flask by incubating a 1/50,000 dilution of raw ascites fluid in PBS overnight at 4°C followed by three rinses with PBS.

Polyclonal Cell Lines

HDAC7 constructs were cloned into HIV-1 (provided by D. Trono, University of Geneva) or MSCV-based retroviral vectors (Hawley et al., 1994). These vectors allow simultaneous expression of HDAC7 and eGFP by using an internal ribosome entry site. Production of HIV-derived particles was performed as described (Jordan et al., 2001). MSCV recombinant retroviruses were obtained by transfection of retroviral vector plasmids into ecotropic virus-packaging cells (BOSC23) (Pear et al., 1993). DO11.10 cells (0.5×10^6) were spin infected for 2 hr at 2400 rpm in 2 ml of viral stock containing polybrene at 4 μg/ml (Pear et al., 1993). The cells were allowed to recover for 24–48 hr, and GFP-expressing cells (~30%) were sorted by flow cytometry and expanded for further analysis. The percentage of GFP-positive cells was stable over time and typically above 98%.

For cell death assay, phycoerythrin (PE)-coupled annexin V (Pharmingen) was used following the manufacturer's recommendations. Cell viability was also confirmed by propidium iodide (PI) exclusion assay.

Flow Cytometry and RT-PCR

Postnatal human thymus specimens were obtained from patients undergoing cardiac surgery (Moffitt Hospital at University of California, San Francisco) and were processed within 6 hr. After mechanical disruption of thymus fragments, single-cell suspensions of thymocytes were stained with a mAb cocktail containing CD4-PE (Becton Dickinson), CD8-Tricolor (Becton Dickinson), and CD3-FITC (Becton Dickinson). A FACS Vantage (Becton Dickinson) was used to purify five thymocyte subsets: $CD3^+CD4^+CD8^-$ (SP4), $CD3^+CD4^-CD8^+$ (SP8), $CD3^{low}CD4^+CD8^+$ (DP^{low}), $CD3^{med/high}CD4^+CD8^+$ ($DP^{med/high}$), and $CD3^-CD4^-CD8^-$ (TN). Typically, the purity of sorted cells was greater than 97%. Thymocyte subpopulations were frozen as dry pellets and stored at 80°C for RNA extraction. Total RNA was extracted from frozen pellets (~10^5 cells) with Trizol (Gibco BRL) according to the manufacturer's instructions. RNA was treated with DNaseI (RQ1 Rnase-Free Dnase, Promega) to ensure total removal of genomic DNA. First-strand cDNA (20 μl) was generated from isolated RNA with the SuperScript First-Strand Synthesis System for RT-PCR (Gibco BRL) as described by the manufacturer. HDAC mRNAs were quantified with the TaqMan fluorogenic detection system on an ABI Prism 7700 Sequence Detector (Perkin-Elmer Applied Biosystems). PCR reactions were performed in duplicate on two dilutions of first strand cDNA with the following primers: HDAC4 forward 5′-TGACCGCCATTTGCGA-3′, HDAC4 reverse 5′-CGTTTC CCAGCAAGGCA-3′, HDAC5 forward 5′-TGGTCTACGACACGTT CATGCT-3′, HDAC5 reverse 5′-TCAGGGTGCACGTGTGTGTT-3′, HDAC7 forward 5′-TGGTGTCTGCTGGATTTGATG-3′, HDAC7 reverse 5′-ATCCAAAACATTTGGCAGAAACAT-3′. MGB-5′-CCTCGGA AGCATGTGTTA-3′, MGB-5′-CACCAGTGCATGTGC-3′, and FAM-5′-CCGGCCCCACTGGGTGGCTA-3′TAMRA (Operon, CA) were used as HDAC4, HDAC5, and HDAC7-specific probe, respectively. PCR amplification consisted of denaturation at 95°C for 10 min, followed by 40 cycles of denaturation at 95°C for 15 s and annealing/extension at 58°C for HDAC7 or 60°C for HDAC4/5 for 60 s. For GAPDH detection, the TaqMan GAPDH control reagents kit (Applied Biosystems, CA) was used with an annealing/extension step at 60°C. Standard curves were plotted for HDACs and GAPDH. For each sample, HDAC expression was normalized to GAPDH.

For CD69 and CD25 expression studies, a polyclonal cell line overexpressing HDAC7 was stimulated with PMA/ionomycin. After 2 (CD69) and 8 hr (CD25) of treatment, cells were stained with the corresponding PE-coupled monoclonal antibodies (Pharmingen) and analyzed by flow cytometry using a FACScan cytometer (Beckton Dickinson)

Northern Blot Analysis

The tissue expression of HDAC7 was analyzed with a multiple human tissue Northern blot and RNA master blots from Clontech. For TSA treatment, DO11.10 cells were treated with 400 nM TSA (Sigma) for various times. Total RNA (5 μg) isolated with Trizol was used to detect the Nur77 message by standard Northern blot analysis (Sambrook et al., 1989). ^{32}P-labeled probes corresponding to human HDAC7, mouse Nur77, or human GAPDH were prepared with the Megaprime DNA labeling system (Amersham Pharmacia Biotech). Blots were prehybridized and hybridized with ExpressHyb hybridization solution (Clontech) and washed under high stringency conditions (Sambrook et al., 1989). Autoradiographs were analyzed with a FUJIX BAS1000 phosphor imaging system (Fuji, Tokyo, Japan).

In Situ Hybridization

In situ hybridization was performed according to Mannheim (1996). Sense and antisense digoxigenin-labeled human HDAC7 riboprobes were prepared with the Dig RNA Labeling Kit (Boehringer Mannheim) and shortened to 150–300 base fragments by alkaline hydrolysis. Sections of formalin-fixed paraffin-embedded tissue (4 μm thick) were deparaffinized, hydrated, pretreated with 0.2N HCl for 10 min and digested with proteinase K (Dako) for 25 min. The tissue was covered with probe solution (0.5 ng/μl) and hybridized overnight at 55°C. Excess probe was removed by stringent washes with: 5× SSC for 30 min at 37°C, 50% formamide/50% 2× SSC for 20 min at 55°C,

2× SSC for 15 min at 42°C, and 0.1× SSC for 15 min at 42°C. The sections were incubated with anti-digoxigenin Fab fragments conjugated with alkaline phosphatase diluted 1:300 (Boehringer Mannheim) for 30 min, followed by the substrate BCIP/NBT (Vector Laboratories, Burlingame, CA) and developed overnight. The slides were washed and then counterstained with Nuclear Fast Red (Vector Laboratories).

Immunoprecipitation

Total cellular extracts from DO11.10 cells or primary thymocytes were prepared in IPLS buffer (Fischle et al., 1999) supplemented with protease inhibitors (Complete, Roche Molecular Biochemicals, IN). Immunoprecipitations were carried out overnight at 4°C. For FLAG-tagged proteins, M2-agarose (Sigma) antibody was used at 15 μl/ml. For immunoprecipitation of endogenous HDAC7, anti-HDAC7 antiserum was used at approximately 10 μg/ml in combination with 20 μ/ml preblocked (10 mg/ml bovine serum albumin) 50% protein G-Sepharose slurry (Amersham Pharmacia Biotech). Immunoprecipitated material was washed three times in IPLS and three times in IPLS containing 1 M NaCl (Fischle et al., 1999). Bound proteins were subjected to SDS-PAGE and Western blotting analysis.

Immunofluorescence

D011.10 cells transfected with HDAC7-GFP-fusion contructs were stimulated with PMA/ionomycin or α-CD3 antibody. Localization of the proteins was assessed by real-time immunofluorescence microscopy.

SDS-PAGE and Western Blotting

SDS-PAGE and Western blot analysis were performed according to standard procedures (Sambrook et al., 1989). Western blots were developed with the ECL detection kit (Amersham Pharmacia Biotech). Anti-HDAC7, anti-FLAG, and anti-actin antibodies were purchased from Santa Cruz Biotechnology (Santa Cruz, CA). Anti-mouse Nur77 and anti-MEF2D antibodies were from BD Pharmingen (San Diego, CA).

GST Fusion Proteins, In Vitro Translation, and Pull-Down Assays

These assays were performed as reported (Fischle et al., 2002).

Chromatin Immunoprecipitation Assays

Chromatin was prepared as described (Orlando et al., 1997) with several modifications. DO11.10 cells were activated with PMA and ionomycin. After 0, 1, 2 and 4 hr of treatment, cells were treated with 1% formaldehyde at room temperature. After 10 min, glycine was added to 0.125 M to stop crosslinking, and the cells were lysed in a buffer A (10 mM Tris-HCl [pH 7.4], 10 mM NaCl, 3 mM MgCl2, 0.3 M sucrose, 10 mM Na butyrate) containing protease inhibitors and 0.1% NP-40. Nuclei were pelleted in buffer A supplemented with 10 mM CaCl2 and digested with micrococcal nuclease to obtain chromatin fragments with an average size of 500 base pairs. Soluble chromatin was released from nuclei by brief sonication and cleared by centrifugation. Chromatin solutions were supplemented with 0.5% sarcosyl, purified by isopicnic centrifugation on cesium chloride gradients, and stored at –70°C.

Immunoprecipitations were done overnight at 4°C with 5 μg of anti-acetylated histone H3 (Upstate Biotechnology, Lake Placid, NY) in immunoprecipitation (IP) buffer (10 mM Tris [pH 8], 1 mM EDTA, 1% Triton X 100, 0.1% sodium deoxycholate, 0.1% SDS, 150 mM NaCl). Immune complexes were collected with protein A-agarose preblocked with sonicated salmon sperm DNA and bovine serum albumin (Upstate Biotechnology). Immunoprecipitates were washed three times in washing buffer (IP buffer supplemented with 0.1 mg/ml yeast tRNA) and three times in washing buffer containing 500 mM NaCl. Immune complexes were eluted with 1% SDS and 100 mM NaHCO3. Formaldehyde crosslinks were reversed by incubating the samples with 200 mM NaCl at 65°C overnight. The immunoprecipitated DNA was purified by proteinase K treatment, phenol:chloroform extractions, and ethanol precipitation. Immunoprecipitated DNA and input (nonimmunoprecipitated) chromatin were analyzed by PCR using the following primer pair for Nur77 promoter detection (5′-AGGGGGAGGAGATCCTGTTC-3′ and 5′-ATTGACGCAGGGAG CGCGGAT-3′). Amplification products were run on a polyacrylamide gel and detected with a FUJIX BAS1000 phosphor imaging system (Fuji, Tokyo, Japan).

Generation of HDAC7-Deficient DO11.10 Cells

MSCV-H1-GFP was constructed by inserting a human H1 promoter-terminator cassette into MSCV Puro (Clontech) and replacing the puromycin resistance gene with GFP. Sequences encoding shRNAs targeted to either mouse HDAC7 (target sequence: AGACAAGAG CAAGCGAAGt) or GL3 luciferase (target sequence: CTTACGCT GAGTACTTCGA) were ligated into MSCV H1 GFP to generate MSCV-H1-GFP/HDAC7 and MSCV-H1-GFP/GL3. DO11.10 cells were spin infected for 2 hr with MSCV-H1-GFP/HDAC7 or MSCV-H1-GFP/GL3 three times at 24 hr intervals. Twenty-four hours after the last infection (80% cells GFP-positive), cells exhibiting highest GFP fluorescence, ~10% of the total cell population, were isolated by FACS. Cells were expanded and characterized as described in the text.

Acknowledgments

We thank John C.W. Carroll and Stephen Gonzales for graphics, Heather Gravois for manuscript preparation, Stephen Ordway and Gary Howard for editorial assistance, and Astar Winoto and Didier Trono for reagents. We thank Kavhe Bastani and Mike McCune for discussions, Christophe Kreiss for help with TaqMan analysis, and Jason Barber for statistical analysis. This work was supported in part by NIH grant GM51671 and by institutional funds from the Gladstone Institute of Virology and Immunology (E.V.). F.D. is a research associate from the Belgian National Fund of Scientific Research and was supported in part by a fellowship from the International Agency for Research on Cancer. W.F. was supported in part by a fellowship from the Boehringer Ingelheim Foundation, Germany.

Received: July 3, 2002
Revised: February 27, 2003
Accepted: March 25, 2003
Published: May 14, 2003

References

Calnan, B.J., Szychowski, S., Chan, F.K., Cado, D., and Winoto, A. (1995). A role for the orphan steroid receptor Nur77 in apoptosis accompanying antigen-induced negative selection. Immunity *3*, 273–282.

Dressel, U., Bailey, P.J., Wang, S.C., Downes, M., Evans, R.M., and Muscat, G.E. (2001). A dynamic role for HDAC7 in MEF2-mediated muscle differentiation. J. Biol. Chem. *276*, 17007–17013.

Esau, C., Boes, M., Youn, H.D., Tatterson, L., Liu, J.O., and Chen, J. (2001). Deletion of calcineurin and myocyte enhancer factor 2 (MEF2) binding domain of Cabin1 results in enhanced cytokine gene expression in T cells. J. Exp. Med. *194*, 1449–1459.

Fischle, W., Emiliani, S., Hendzel, M.J., Nagase, T., Nomura, N., Voelter, W., and Verdin, E. (1999). A new family of human histone deacetylases related to Saccharomyces cerevisiae HDA1p. J. Biol. Chem. *274*, 11713–11720.

Fischle, W., Kiermer, V., Dequiedt, F., and Verdin, E. (2001b). The emerging role of class II histone deacetylases. Biochem. Cell Biol. *79*, 337–348.

Fischle, W., Dequiedt, F., Fillion, M., Hendzel, M.J., Voelter, W., and Verdin, E. (2001a). Human HDAC7 histone deacetylase activity is associated with HDAC3 in vivo. J. Biol. Chem. *276*, 35826–35835.

Fischle, W., Dequiedt, F., Hendzel, M.J., Guenther, M.G., Lazar, M.A., Voelter, W., and Verdin, E. (2002). Enzymatic activity associated with class II HDACs is dependent on a multiprotein complex containing HDAC3 and SMRT/N-CoR. Mol. Cell *9*, 45–57.

Grozinger, C.M., and Schreiber, S.L. (2000). Regulation of histone deacetylase 4 and 5 and transcriptional activity by 14-3-3-dependent cellular localization. Proc. Natl. Acad. Sci. USA *97*, 7835–7840.

Hawley, R.G., Lieu, F.H., Fong, A.Z., and Hawley, T.S. (1994). Versatile retroviral vectors for potential use in gene therapy. Gene Ther. *1*, 136–138.

Jordan, A., Defechereux, P., and Verdin, E. (2001). The site of HIV-1

integration in the human genome determines basal transcriptional activity and response to Tat transactivation. EMBO J. *20*, 1726–1738.

Kao, H.Y., Verdel, A., Tsai, C.C., Simon, C., Juguilon, H., and Khochbin, S. (2001). Mechanism for nucleocytoplasmic shuttling of histone deacetylase 7. J. Biol. Chem. *276*, 47496–47507.

Kasler, H.G., Victoria, J., Duramad, O., and Winoto, A. (2000). ERK5 is a novel type of mitogen-activated protein kinase containing a transcriptional activation domain. Mol. Cell. Biol. *20*, 8382–8389.

Khochbin, S., Verdel, A., Lemercier, C., and Seigneurin-Berny, D. (2001). Functional significance of histone deacetylase diversity. Curr. Opin. Genet. Dev. *11*, 162–166.

Liu, Z.G., Smith, S.W., McLaughlin, K.A., Schwartz, L.M., and Osborne, B.A. (1994). Apoptotic signals delivered through the T-cell receptor of a T-cell hybrid require the immediate-early gene nur77. Nature *367*, 281–284.

Mannheim, B. ed. (1996). Nonradioactive *In Situ* Hybridization Application Manual, Second Edition. Roche Diagnostic Corporation. http://www.roche-applied-science.com/prod_inf/manuals/InSitu/InSi_toc.htm.

Martin, J.F., Miano, J.M., Hustad, C.M., Copeland, N.G., Jenkins, N.A., and Olson, E.N. (1994). A Mef2 gene that generates a muscle-specific isoform via alternative mRNA splicing. Mol. Cell. Biol. *14*, 1647–1656.

McKinsey, T.A., Zhang, C.L., Lu, J., and Olson, E.N. (2000a). Signal-dependent nuclear export of a histone deacetylase regulates muscle differentiation. Nature *408*, 106–111.

McKinsey, T.A., Zhang, C.L., and Olson, E.N. (2000b). Activation of the myocyte enhancer factor-2 transcription factor by calcium/calmodulin-dependent protein kinase-stimulated binding of 14-3-3 to histone deacetylase 5. Proc. Natl. Acad. Sci. USA *97*, 14400–14405.

McKinsey, T.A., Zhang, C.L., and Olson, E.N. (2001a). Control of muscle development by dueling HATs and HDACs. Curr. Opin. Genet. Dev. *11*, 497–504.

McKinsey, T.A., Zhang, C.L., and Olson, E.N. (2001b). Identification of a signal-responsive nuclear export sequence in class II histone deacetylases. Mol. Cell. Biol. *21*, 6312–6321.

McKinsey, T.A., Zhang, C.L., and Olson, E.N. (2002). MEF2: a calcium-dependent regulator of cell division, differentiation and death. Trends Biochem. Sci. *27*, 40–47.

Miska, E.A., Langley, E., Wolf, D., Karlsson, C., Pines, J., and Kouzarides, T. (2001). Differential localization of HDAC4 orchestrates muscle differentiation. Nucleic Acids Res. *29*, 3439–3447.

Orlando, V., Strutt, H., and Paro, R. (1997). Analysis of chromatin structure by in vivo formaldehyde cross-linking. Methods *11*, 205–214.

Pear, W.S., Nolan, G.P., Scott, M.L., and Baltimore, D. (1993). Production of high-titer helper-free retroviruses by transient transfection. Proc. Natl. Acad. Sci. USA *90*, 8392–8396.

Sambrook, J., Fritsch, E.F., and Maniatis, T. (1989). Molecular Cloning: A Laboratory Manual, Second Edition (Cold Spring Harbor, NY: Cold Spring Harbor Laboratory Press).

Strahl, B.D., and Allis, C.D. (2000). The language of covalent histone modifications. Nature *403*, 41–45.

Van Lint, C., Emiliani, S., and Verdin, E. (1996). The expression of a small fraction of cellular genes is changed in response to histone hyperacetylation. Gene Expr. *5*, 245–253.

Wang, A.H., Kruhlak, M.J., Wu, J., Bertos, N.R., Vezmar, M., Posner, B.I., Bazett-Jones, D.P., and Yang, X.-J. (2000). Regulation of histone deacetylase 4 by binding of 14-3-3 proteins. Mol. Cell. Biol. *20*, 6904–6912.

Woronicz, J.D., Calnan, B., Ngo, V., and Winoto, A. (1994). Requirement for the orphan steroid receptor Nur77 in apoptosis of T-cell hybridomas. Nature *367*, 277–281.

Woronicz, J.D., Lina, A., Calnan, B.J., Szychowski, S., Cheng, L., and Winoto, A. (1995). Regulation of the Nur77 orphan steroid receptor in activation-induced apoptosis. Mol. Cell. Biol. *15*, 6364–6376.

Youn, H.D., Sun, L., Prywes, R., and Liu, J.O. (1999). Apoptosis of T cells mediated by Ca2+-induced release of the transcription factor MEF2. Science *286*, 790–793.

Youn, H.D., and Liu, J.O. (2000). Cabin1 represses MEF2-dependent Nur77 expression and T cell apoptosis by controlling association of histone deacetylases and acetylases with MEF2. Immunity *13*, 85–94.

Youn, H.D., Chatila, T.A., and Liu, J.O. (2000a). Integration of calcineurin and MEF2 signals by the coactivator p300 during T-cell apoptosis. EMBO J. *19*, 4323–4331.

Youn, H.D., Grozinger, C.M., and Liu, J.O. (2000b). Calcium regulates transcriptional repression of myocyte enhancer factor 2 by histone deacetylase 4. J. Biol. Chem. *275*, 22563–22567.

Zhang, C.L., McKinsey, T.A., and Olson, E.N. (2001). The transcriptional corepressor MITR is a signal-responsive inhibitor of myogenesis. Proc. Natl. Acad. Sci. USA *98*, 7354–7359.

Zhou, X., Marks, P.A., Rifkind, R.A., and Richon, V.M. (2001). Cloning and characterization of a histone deacetylase, HDAC9. Proc. Natl. Acad. Sci. USA *98*, 10572–10577.